

Strangeness production in $\sqrt{s_{NN}} = 200$ GeV Au+Au collisions at RHIC

Jens Ivar Jørdre⁹

for the BRAHMS Collaboration:

I. Arsene¹⁰, I. G. Bearden⁷, D. Beavis¹, C. Besliu¹⁰, B. Budick⁶, H. Bøggild⁷, C. Chasman¹, C. H. Christensen⁷, P. Christiansen⁷, J. Cibor³, R. Debbé¹, E. Enger¹², J. J. Gaardhøje⁷, M. Germinario⁷, K. Hagel⁸, O. Hansen⁷, A. Holm⁷, H. Ito^{1,11}, A. Jipa¹⁰, F. Jundt², J. I. Jørdre⁹, C. E. Jørgensen⁷, R. Karabowicz⁴, E. J. Kim¹, T. Kozik⁴, T. M. Larsen¹², J. H. Lee¹, Y. K. Lee⁵, S. Lindal¹², R. Lystad⁹, G. Løvholden¹², Z. Majka⁴, A. Makeev⁸, B. McBreen¹, M. Mikelsen¹², M. Murray^{8,11}, J. Natowitz⁸, B. Neumann¹¹, B. S. Nielsen⁷, J. Norris¹¹, D. Ouerdane⁷, R. Planeta⁴, F. Rami², C. Ristea¹⁰, O. Ristea¹⁰, D. Röhrich⁹, B. H. Samset¹², D. Sandberg⁷, S. J. Sanders¹¹, R. A. Scheetz¹, P. Staszé^{4,7}, T. S. Tveter¹², F. Videbæk¹, R. Wada⁸, Z. Yin⁹, and I. S. Zgura¹⁰

¹ Brookhaven National Laboratory, Upton, New York 11973, USA

² Institut de Recherches Subatomiques, Université Louis Pasteur, Strasbourg, France

³ Institute of Nuclear Physics, Krakow, Poland

⁴ Smoluchowski Inst. of Physics, Jagiellonian University, Krakow, Poland

⁵ Johns Hopkins University, Baltimore 21218, USA

⁶ New York University, New York 10003, USA

⁷ Niels Bohr Institute, Blegdamsvej 17, University of Copenhagen, 2100 Copenhagen, Denmark

⁸ Texas A&M University, College Station, Texas, 17843, USA

⁹ Department of Physics, University of Bergen, Bergen, Norway

¹⁰ University of Bucharest, Romania

¹¹ University of Kansas, Lawrence, Kansas 66045, USA

¹² Department of Physics, University of Oslo, Oslo, Norway

Received: date / Revised version: date

Abstract. The BRAHMS collaboration has measured identified particle spectra from $Au + Au$ collisions at $\sqrt{s_{NN}} = 200$ GeV. Rapidity densities are deduced from fits to the pion and kaon spectra. dN/dy is plotted as a function of rapidity and 4π yields and ratios are calculated. The signed K/π ratios are compared to values obtained at lower energies. We find that K^-/π^- increases monotonically from the AGS and SPS regimes, while K^+/π^+ is similar to what was found at the highest $\sqrt{s_{NN}}$ at SPS.

PACS. 25.75.Dw Particle and resonance production

1 Introduction

At the Relativistic Heavy Ion Collider (RHIC) nuclear matter is studied under conditions that are among the most extreme yet obtained in a laboratory. These conditions are reached by colliding gold nuclei at an energy of $\sqrt{s_{NN}} = 200$ GeV. The ultimate goal is to produce a Quark Gluon Plasma (QGP), a phase of the nuclear matter which from lattice QCD calculations is predicted to occur at high temperature[1,2]. In this phase the quarks and gluons, bound within nucleons at lower energies, are deconfined and partonic degrees of freedom have to be considered.

As the produced QGP will only exist for a few fm/c it is not detectable, and signatures of its creation need to be found in the hadronic products of the collision. In particular an increase in production of strange particles

has been proposed as one of the potential probes for a QGP[3].

A large portion of the produced strangeness is carried by kaons. Therefore an understanding of the kaon production mechanism and dynamic behavior in the collision is important for developing the strangeness picture.

2 Experimental setup and analysis

The BRAHMS experiment is unique in its ability to identify charged particles over a broad range in rapidity and transverse momentum. It covers a rapidity window from mid-rapidity around $y \sim 0$ to the forward region around $y \sim 3$. Its p_T coverage depends on particle species as well as spectrometer setting.

The BRAHMS experimental setup consists of two spectrometer arms, each of interleaved tracking detectors and magnets. The mid-rapidity spectrometer (MRS) has two TPCs and one magnet. The forward spectrometer (FS) uses two TPCs and three drift chambers for tracking and has four dipole magnets. The MRS has a time of flight wall for particle identification, while the FS uses time of flight for low momentum particles and Cherenkov detectors for high momentum particle identification.

There are also detectors for characterizing the events in terms of centrality and vertex position. Plastic scintillator tiles and silicon strip detectors surround the nominal interaction vertex at close distance for centrality determination. On either side of the vertex Cherenkov radiator beam-beam counters are placed, giving vertex as well as centrality information. Even further away are zero-degree calorimeters which detect spectator neutrons. (For a more detailed description of the experimental setup see [4].)

The spectrometer arms cover small solid angles at a given setting. Data from many angular and magnetic field settings are therefore combined to generate spectra. The data is thereafter corrected for acceptance as well as decay, multiple scattering and detector efficiencies. Feed down corrections from the decay of hyperons and resonances have not been applied to the present results. The errors indicated on the included plots are statistical only. A discussion on the systematical errors can be found in [5]. The systematical uncertainty for the rapidity densities is typically estimated to be around 5% or less for both pions and kaons.

3 Results and discussion

BRAHMS has identified kaons and pions at various rapidities. Spectra of identified kaons are shown in Fig. 1. For most rapidity settings they cover the mean p_T . This study was done for the 5% most central collisions. The range of the spectra therefore indicate the acceptance in p_T for each rapidity region. Similar spectra were deduced for pions.

Fitting the spectra for pions with a power law in p_T and for kaons with an exponential in m_T we are able to extrapolate outside of the experimental range to deduce a rapidity density of dN/dy . The resulting rapidity densities as functions of rapidity are shown in Fig. 2. These densities are subsequently fitted with single Gaussians.

As seen in Fig. 2 the selected fit function describe the rapidity density closely. Integrating them over the whole rapidity range we obtain the first 4π yields at RHIC energies. Results from the fits are listed in Tab. 1. Also given are the 4π signed K/π ratios.

Because a large fraction of the strangeness is carried by kaons, it is interesting to compare the relative yield of strange to non-strange particles. The increase in strangeness production may be gauged to some extent from these results, although a full understanding will require studies of the hyperons and other resonances that carry strangeness in the reaction. Fig. 3 shows the signed ratio of kaons to pions as a function of center of mass energy from the

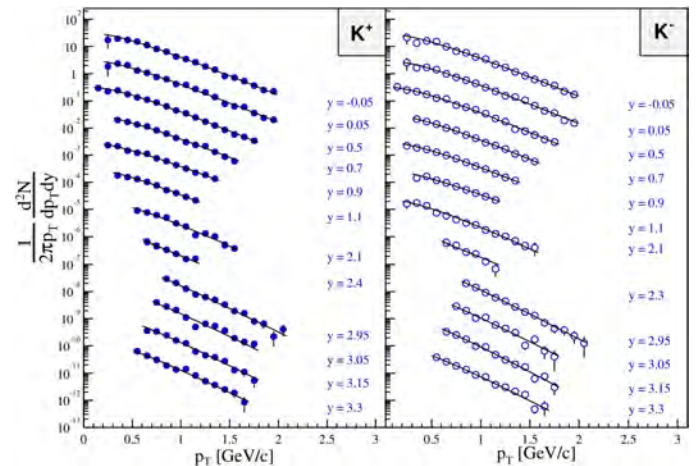


Fig. 1. Kaon spectra at various rapidities. Each spectrum fitted with an exponential in m_T and scaled by 10^{-1} relative to the one above.

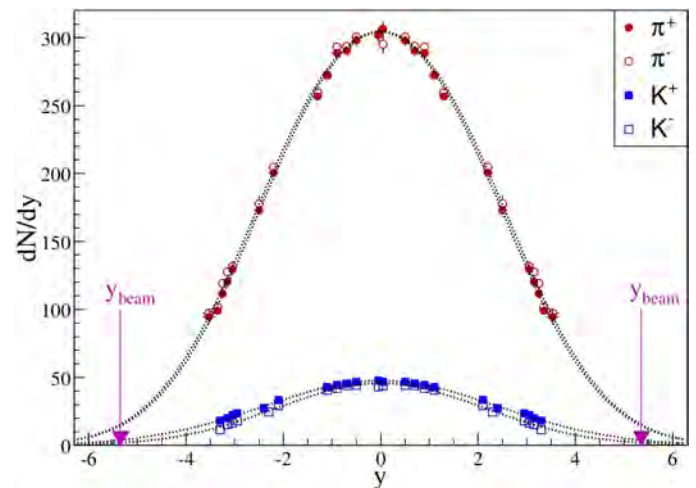


Fig. 2. dN/dy for π^\pm and K^\pm as deduced from extrapolated yields at the various rapidities. Note that BRAHMS measures only at positive rapidities.

Table 1. 4π yields and signed ratios of π^\pm and K^\pm .

particle	4π yield	4π ratio
K^+	286 ± 4	} $16.3\% \pm 0.3\%$
π^+	1755 ± 11	
K^-	243 ± 2	} $13.5\% \pm 0.2\%$
π^-	1796 ± 12	

AGS energy regime, through the SPS energies, and to the top RHIC energy. At mid-rapidity the positive and negative ratios appear to approach each other at higher energies and converge to a value of around 15%. The same general trend is also seen for the 4π ratios. The difference between positive and negative ratios integrated over the full phase space and the mid-rapidity results should then be attributed to differences at forward rapidities, as may also be inferred from like particle ratios in [6].

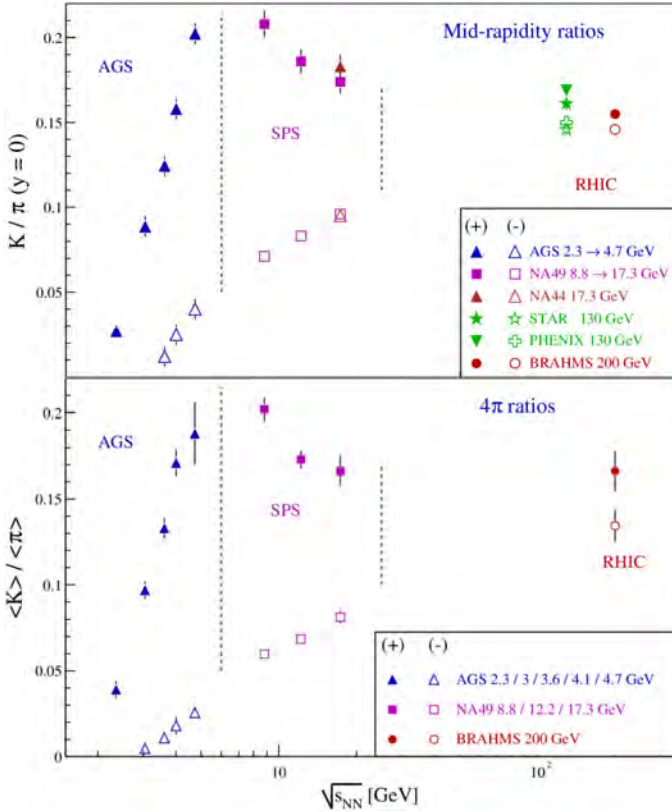


Fig. 3. K/π at mid-rapidity (upper panel) and K/π integrated over the full phase space as a function of center of mass energy. The AGS points are from [7–9], the ones for SPS from [10, 11] and supplemental RHIC points from [12–14].

Particle yields in heavy ion collisions at mid-rapidity and from full phase space integrations have been analyzed within the thermal model from SIS energies up to the SPS regime [15]. Within this framework we plot K^-/K^+ as a function of \bar{p}/p (Fig. 4), where the BRAHMS proton results are obtained in a similar manner as described for the π and K data. (See [16] for details on p and \bar{p} .) The kaons and (anti-)protons are measured at slightly different rapidities, and the kaon points are therefore interpolations to the p and \bar{p} rapidities.

Fig. 4 shows the charge conjugate ratio of kaons to that of protons obtained at RHIC, as well as results from AGS and SPS. Simply counting the number of included quarks one would expect $K^-/K^+ = (\bar{p}/p)^{1/3}$, shown as the dotted curve in the figure. The AGS and SPS points are clearly not described by this curve. The thermal model curve, which includes a strangeness suppression factor and is shown as the solid line, is in better agreement with all of the data points.

One could, however, question the comparison of the BRAHMS data points to the theoretical predictions since our data are measured at various rapidities and are not integrated over the full phase space. We have also not included possible isospin effects [17]. Despite these caveats, we find an intriguing correlation between our ratios and those of the thermal model.

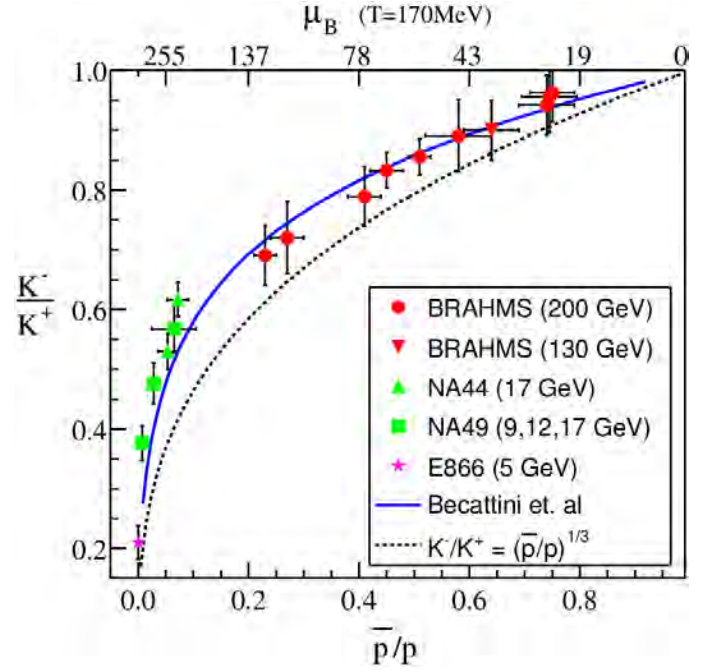


Fig. 4. Ratio of kaons as a function of \bar{p}/p or baryonic chemical potential.

4 Conclusions

In conclusion the BRAHMS experiment has identified hadrons over a broad range of phase space. We show yields and ratios integrated over 4π solid angle for pions and kaons. The K^-/π^- ratio vs. center of mass energy follows the trend of steady increase previously seen at lower energies, while K^-/K^+ appears to become saturated at high $\sqrt{s_{NN}}$. We find that K^-/K^+ vs \bar{p}/p measured in various rapidity regions follows thermal model predictions for the same ratio integrated over the full phase.

References

1. F. Karsch, Nucl. Phys. **A689**, (2002) 199
2. Z. Fodor, S. D. Katz, Heavy Ion Phys. **18**, (2003) 41-48
3. J. Rafelski, B. Müller, Phys. Rev. Lett. **48**, (1982) 1066
4. M. Adamczyk *et al.*, Nucl. Inst. Meth. **A499**, (2003) 437
5. D. Ouerdane, Ph.D. thesis, (2003) Niels Bohr Institute, Denmark
6. I. G. Bearden *et al.*, Phys. Rev. Lett. **90**, (2003) 102301
7. J. L. Klay *et al.*, nucl-ex/0306033
8. L. Ahle *et al.*, Phys. Rev. C **60**, (1999) 044904
9. L. Ahle *et al.*, Phys. Lett. B **490**, (2000), 53
10. S. V. Afanasiev *et al.*, Phys. Rev. C **66**, (2002) 054902
11. I. G. Bearden *et al.*, Phys. Lett. B **471**, (1999) 6
12. C. Adler *et al.*, nucl-ex/0206008
13. O. Barannikova and F. Wang, Nucl. Phys. A **715**, (2003) 458c-461c
14. K. Adcox *et al.*, Phys. Rev. Lett. **88**, (2002) 242301
15. F. Becattini *et al.*, Phys. Rev. C **64**, (2001) 024901
16. P. H. L. Christiansen, Ph.D. thesis, (2003) Niels Bohr Institute, Denmark
17. H. G. Fischer, Nucl. Phys. A **715**, (2003) 118c-128c